

## Magnetic Moment Distribution in Ferromagnetic Co-Mn Alloys\*

T. J. Hicks and A. R. Wildes

Department of Physics, Monash University,  
Clayton, Vic. 3168, Australia.

### Abstract

Using the magnetic environment model, the moment distributions for ferromagnetic  $\text{Co}_{1-x}\text{Mn}_x$  alloys in the composition range ( $0 < x < 0.25$ ) were calculated from the mean saturating moments of the alloys. The calculation also gives the mean moment of each species as a function of concentration. The predictions correspond extremely well with the existing experimental data. In particular, the increase in the correlation length close to the ferromagnetic critical concentration is clear in the cross section data and model.

### 1. Introduction

The reasons for the formation and coupling of magnetic moments in metallic systems have been actively pursued for many years. In 3d transition metal alloys the unpaired electrons form a common band, leading to non-integral values (in Bohr magnetons) of the atomic magnetic moments. The direct approach to this problem is to calculate the band structure within an approximation like the coupled pair approximation (CPA) and the spin density functional theory in the 'local density' approximation (LDA). An example of this approach is that of Johnson *et al.* (1985) for a disordered Fe-Ni alloy. Some understanding of the ferromagnetism of these alloy systems can be obtained more simply from the application of phenomenological models of the moment distribution. Of these, the magnetic environment model (Hicks 1980) can cope with the approach to the ferromagnetic critical concentration, and seems particularly appropriate for the Co-Mn alloy system, which is the subject of this paper and has a ferromagnetic critical concentration of 30 at.% Mn.

Magnetic studies (Crangle 1957; Kouvel 1960) of cobalt-rich fcc  $\text{Co}_{1-x}\text{Mn}_x$  alloys have revealed a ferromagnetic phase whose Curie temperature steadily decreases with increasing manganese concentration. This phase disappears at around 30 at.% Mn and the system shows a clear antiferromagnetic phase at  $x > 0.42$  (Men'shikov *et al.* 1985). The composition range that lies between these two phases (i.e.  $0.25 < x < 0.42$ ), however, has not been clearly understood until recently.

\* Paper presented at the Festschrift Symposium for Dr Geoffrey Fletcher, Monash University, 11 December 1992.

In 1960 Kouvel investigated the susceptibility data and hysteresis loops of these alloys in the composition range  $0.25 < x < 0.373$ . From these data and previous measurements (Crangle 1957) he calculated ferromagnetic and paramagnetic moments for the compositions  $0 < x < 0.373$ . The paramagnetic moments were taken from the Curie constant at high temperatures. He concluded that the ferromagnetic moment approached zero at approximately 30 at.% Mn. The paramagnetic moment, however, increased with increasing Mn concentration to become approximately  $3\mu_B$  at 37.3 at.% Mn.

The existence of such a large paramagnetic moment on each atom was disproved by Wildes *et al.* in 1992. Using neutron diffraction with polarisation analysis Wildes *et al.* searched for the large diffuse magnetic cross section that would be apparent if such moments existed. No such cross section was observed, as is evident in Fig. 1 which shows the large discrepancy between the expected cross section and the measured cross section. The expected cross section was calculated using the paramagnetic moment determined by Kouvel to find the mean spin,  $\bar{S}$ , in the equation

$$\frac{d\sigma}{d\Omega} = \frac{2}{3} \left( \frac{e^2\gamma}{2mc^2} \right)^2 f^2(\kappa) g^2 \bar{S}(\bar{S}+1) \left\{ 1 + 12\gamma_1 \frac{\bar{S}^2}{\bar{S}(\bar{S}+1)} \frac{\sin(\kappa R_1)}{\kappa R_1} \right\}, \quad (1)$$

where  $\kappa$  is the magnitude of the scattering vector  $\kappa$ . First-neighbour interactions only were assumed and a value of  $\gamma_1$  was calculated to match the susceptibility at 300 K. Wildes *et al.* concluded that the moment on individual atoms is close to zero in the composition range between the ferromagnetic and antiferromagnetic phases, and that large-scale cooperation between diffuse clouds of moments was responsible for the observed susceptibility.

This result is borne out by Cable (1982) who used polarised neutrons without analysis to measure the diffuse cross section of these alloys in the ferromagnetic composition range  $0 < x < 0.25$ . Using the phenomenological linear atomic environment model of Marshall (1968), he was able to determine the average ferromagnetic moment on each species as a function of concentration. Cable found a positive moment on the cobalt and a negative moment on the manganese. Both moments approached zero as  $x$  approached 30 at.% Mn.

This modelling, however, is not ideal. The plot of moment versus concentration for this system clearly shows an increasing first derivative with increasing manganese concentration and a critical concentration for ferromagnetism at about  $x = 0.3$ . The Marshall model is not equipped to deal with the increasing correlation length associated with criticality. The model may be corrected up to a point by taking it to higher order (Balcar and Marshall 1968), a method that soon becomes cumbersome and complicated. As an alternative, the magnetic environment model was developed by Hicks for both one-moment (Hicks 1977) and two-moment (Hicks 1980) systems. The two-moment model has been applied with some success to some Ni alloys (Hicks 1980; Hicks and Moze 1981). A further advantage of this model is its ability to predict diffuse cross sections, thus providing a check of the values obtained for the moments.

By fitting the saturating moment per atom as a function of concentration with the model, we hoped to find the moment of each species of atom as a function of concentration. As a check we hoped to then predict the neutron diffuse cross

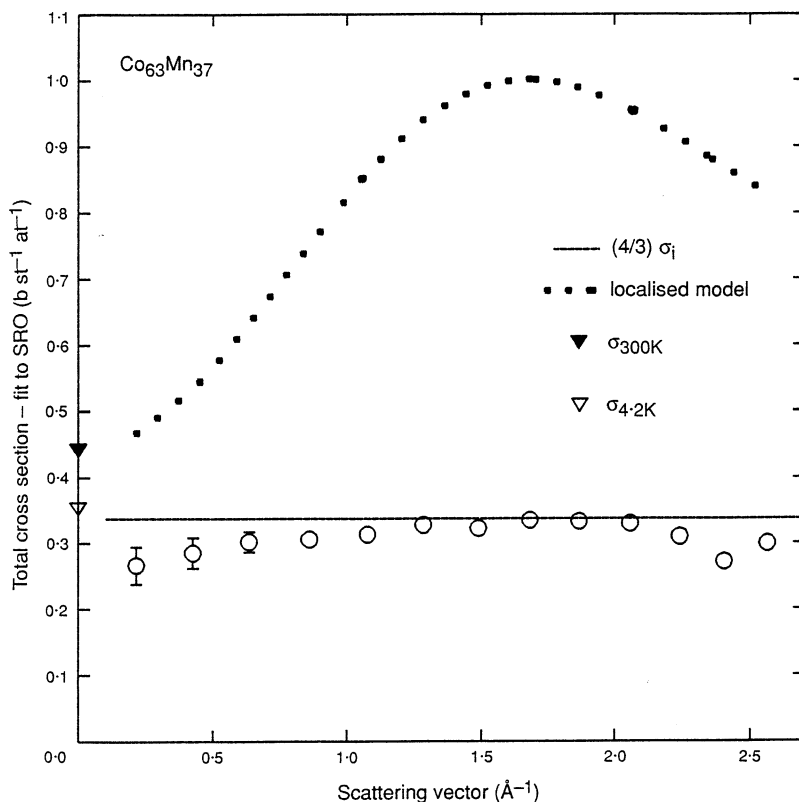


Fig. 1. Comparison between the expected and observed diffuse magnetic cross section in  $\text{Co}_{63}\text{Mn}_{37}$ .

section, which we could then compare with the data obtained by Cable. We have not been completely successful, but what is clear from the following analysis is that the magnetic environment model provides the correct form for the low- $\kappa$  cross sections.

## 2. The Model

The magnetic environment model for a ferromagnetic alloy with two magnetic species (Hicks 1980) is an attempt to model phenomenologically the size of the moments on the atoms as a function of their environment. This follows an earlier phenomenological treatment of the moment distribution (Marshall 1968) in which the moment on each atom is a linear function of the local *atomic occupancy*. The treatment given by Hicks differs from that due to Marshall by introducing, in addition, the effect of the local *magnetic environment* through a local exchange field.

One may assume that  $m(\mathbf{R})$ , the moment on an atom at site  $\mathbf{R}$ , will at first increase linearly with the field at that site, and then asymptote to the saturating moment of that atomic species. In the absence of an external field, any field felt at site  $\mathbf{R}$  will thus be due to an exchange field  $h(\mathbf{R})$ , which may be broken down into a superposition of exchange interactions:

$$\begin{aligned}
h(\mathbf{R}) = & \sum_{\mathbf{R}' \neq \mathbf{R}} m(\mathbf{R}') \{p(\mathbf{R})p(\mathbf{R}')\zeta_1(\mathbf{R}-\mathbf{R}') \\
& + [p(\mathbf{R})(1-p(\mathbf{R}')) + (1-p(\mathbf{R}))p(\mathbf{R}')] \zeta_{12}(\mathbf{R}-\mathbf{R}') \\
& + (1-p(\mathbf{R}))(1-p(\mathbf{R}')) \zeta_2(\mathbf{R}-\mathbf{R}')\}, \tag{2}
\end{aligned}$$

where  $\zeta_1(\mathbf{R}-\mathbf{R}')$  is the exchange interaction between two atoms of type 1 at sites  $\mathbf{R}$  and  $\mathbf{R}'$ ,  $\zeta_2(\mathbf{R}-\mathbf{R}')$  is the exchange interaction between two atoms of type 2, and  $\zeta_{12}(\mathbf{R}-\mathbf{R}')$  is the exchange interaction between an atom of type 1 and an atom of type 2. Here  $p(\mathbf{R})$  is equal to 0 or 1 for type 1 or type 2 atoms respectively.

The simplest form of saturating function (Hicks 1977) is given by  $f(x) = x/(1+x)$ . A point to note is that while this function is the simplest to deal with, it is not ideal. A more realistic saturating function would be odd. However, even the simplest of such functions complicate the algebra and the problem has to be linearised at some later stage (Medina and Cable 1977). Based on the above function, we can write the moment of the atom at site  $\mathbf{R}$  as

$$m(\mathbf{R}) = \frac{\{\alpha_2(\mathbf{R}) + p(\mathbf{R})[\alpha_1(\mathbf{R}) - \alpha_2(\mathbf{R})]\} h(\mathbf{R})}{1 + [B_2 + p(\mathbf{R})(B_1 - B_2)] h(\mathbf{R})}, \tag{3}$$

in which the  $\alpha(\mathbf{R})$ , which are the initial susceptibilities of the two atoms, are assumed to depend linearly on the local *atomic* environment. In this way  $\alpha(\mathbf{R})$  consists of an on-site contribution  $a(0)$  and contributions  $a(\mathbf{R}')$  from neighbouring atoms. The constants  $B_1$  and  $B_2$  are chosen such that the appropriate  $\alpha(\mathbf{R})/B$  is the saturating moment of the atom at  $\mathbf{R}$ .

Equation (3) can be Fourier-transformed and the resulting integral equation solved for the Fourier transform of the moment distribution. This solution is facilitated by writing the Fourier transform of the moment distribution in terms of its average and spatially fluctuating parts:

$$\begin{aligned}
\Xi(\boldsymbol{\kappa}) &= \bar{m} \sum_{\mathbf{R}} \exp(i\boldsymbol{\kappa} \cdot \mathbf{R}) + F(\boldsymbol{\kappa}), \tag{4} \\
F(\boldsymbol{\kappa}) &= \sum_{\mathbf{R}} \exp(i\boldsymbol{\kappa} \cdot \mathbf{R}) (m(\mathbf{R}) - \bar{m}).
\end{aligned}$$

Here  $\bar{m}$  is the mean moment and  $F(\boldsymbol{\kappa})$  is the Fourier transform of the magnetic fluctuations.

Similarly, the atomic distribution can also be written in terms of its average (the concentration  $c$  of species 2) and spatially fluctuating parts

$$\begin{aligned}
P(\boldsymbol{\kappa}) &= c \sum_{\mathbf{R}} \exp(i\boldsymbol{\kappa} \cdot \mathbf{R}) + D(\boldsymbol{\kappa}), \\
D(\boldsymbol{\kappa}) &= \sum_{\mathbf{R}} \exp(i\boldsymbol{\kappa} \cdot \mathbf{R}) (p(\mathbf{R}) - c), \tag{5}
\end{aligned}$$

where  $D(\boldsymbol{\kappa})$  is the Fourier transform of the atomic fluctuations.

The solution of the Fourier transform of (3) can now be separated into a solution for the mean and spatially fluctuating moments (Hicks 1980). We find

$$\bar{m} = \frac{I(0)[a(0) - A(0)] - 1}{BI(0)}, \quad (6)$$

where

$$a(0) = ca_1(0) + (1 - c)a_2(0),$$

$$A(\boldsymbol{\kappa}) = \sum_{\mathbf{R} \neq 0} a(\mathbf{R}) \exp(i\boldsymbol{\kappa} \cdot \mathbf{R}) = c^2 A_1(\boldsymbol{\kappa}) + (1 - c)^2 A_2(\boldsymbol{\kappa}),$$

$$I(\boldsymbol{\kappa}) = \sum_{\mathbf{R} \neq 0} \zeta(\mathbf{R}) \exp(i\boldsymbol{\kappa} \cdot \mathbf{R}) = c^2 I_1(\boldsymbol{\kappa}) + 2c(1 - c)I_{12}(\boldsymbol{\kappa}) + (1 - c)^2 I_2(\boldsymbol{\kappa}),$$

$$B = cB_1 + (1 - c)B_2.$$

For the Fourier transform of the fluctuation of the moment, we find

$$\begin{aligned} F(\boldsymbol{\kappa}) = & \left[ \left\{ \frac{d\bar{m}}{dc} - \left( \frac{dI(0)}{dc} - \frac{dI(\boldsymbol{\kappa})}{dc} \right) [2BI^2(0)]^{-1} \right. \right. \\ & \left. \left. - \left( \frac{dA(0)}{dc} - \frac{dA(\boldsymbol{\kappa})}{dc} \right) (2B)^{-1} \right\} D(\boldsymbol{\kappa}) \right] \\ & \times \left[ 1 + \frac{[I(0) - I(\boldsymbol{\kappa})]}{I^2(0)B\bar{m}} \right]^{-1}. \end{aligned} \quad (7)$$

Here the mean and fluctuating moments are functions of the atomic concentration and the fluctuating part of the atom distribution. These quantities differ from binary alloy to binary alloy because of the statistical nature of the preparation of alloys, but  $c$  and  $D(\boldsymbol{\kappa})$ , and consequently  $\bar{m}$  and  $F(\boldsymbol{\kappa})$ , can be estimated by averaging over an ensemble of identically prepared alloys.

In equation (6)  $\bar{m}$  is the spontaneous moment per atom for a ferromagnetic sample, and this equation can thus be fitted to experimental data for the variation of moment with concentration, using a non-linear least-squares fitting routine. The parameters obtained are combinations of  $a(0)$ ,  $A(\boldsymbol{\kappa})$ ,  $I(\boldsymbol{\kappa})$  and  $B$ . Once these parameters have been optimised, the values of the individual components may be extracted and used to calculate  $F(\boldsymbol{\kappa})$  for any concentration  $c$ . It is convenient to define  $M(\boldsymbol{\kappa})$  by the relation  $F(\boldsymbol{\kappa}) = M(\boldsymbol{\kappa})D(\boldsymbol{\kappa})$ . The function  $M(\boldsymbol{\kappa})$  can be extracted from polarised neutron diffuse scattering results for comparison (Hicks 1980).

The mean moment on each species in the system can be found once  $M(\boldsymbol{\kappa})$  has been calculated. The difference between the two moments is equal to the average of  $M(\boldsymbol{\kappa})$  over all  $\boldsymbol{\kappa}$  (Marshall 1968), which can be calculated approximately by ignoring  $\boldsymbol{\kappa}$ -dependent terms:

$$\bar{m}_1 - \bar{m}_2 = \langle M(\boldsymbol{\kappa}) \rangle \approx \left( \frac{d\bar{m}}{dc} - \frac{1}{2BI^2(0)} \frac{dI(0)}{dc} - \frac{1}{2B} \frac{dA(0)}{dc} \right) \left( 1 + \frac{1}{BI(0)\bar{m}} \right). \quad (8)$$

From this quantity and the average mean moment per atom we may easily separate  $\bar{m}_1$  and  $\bar{m}_2$ .

### 3. Modelling of Co-Mn

Cobalt-rich Co-Mn alloys have both hcp and fcc structures. Thus, particular care was taken in selecting the saturating moments used in the modelling, as we desired to fit the fcc values only. The data used are listed in Table 1.

Table 1. Concentration versus mean moment in the composition range  $0 < x < 0.35$

Mn concentration $x = 1-c$	Mean moment $\bar{m}$	Mn concentration $x = 1-c$	Mean moment $\bar{m}$
0	1.751 <sup>A</sup>	0.198	0.88 <sup>C</sup>
0.02	1.693 <sup>A</sup>	0.200	0.91 <sup>B</sup>
0.338	1.648 <sup>A</sup>	0.23	0.59 <sup>D</sup>
0.0525	1.593 <sup>A</sup>	0.244	0.58 <sup>C</sup>
0.076	1.45 <sup>B</sup>	0.250	0.50 <sup>B</sup>
0.105	1.362 <sup>A</sup>	0.25	0.48 <sup>E</sup>
0.150	1.13 <sup>B</sup>	0.30	0.22 <sup>D</sup>
0.1852	0.983 <sup>A</sup>	0.355	0.00 <sup>D</sup>

<sup>A</sup> Crangle (1957). <sup>B</sup> Nakai *et al.* (1978). <sup>C</sup> Cable (1982). <sup>D</sup> Matsui *et al.* (1970).  
<sup>E</sup> Kouvel (1960).

Fitting equation (6) to these data was not a trivial exercise. The data in Table 1 describe a very simple curve, monotonically decreasing from  $\bar{m} = 1.751\mu_B$  at 0 at.% Mn to  $\bar{m} = 0$  at 30 at.% Mn, and could probably be fitted with a simple quadratic. Equation (6), on the other hand, is a very complicated function. Indeed, we are attempting to fit eight parameters here with a variety of  $c$  dependences. It is worth noting that were this a one-moment system, the number of parameters to fit would decrease to three (Hicks 1977)—a far easier problem. As it is, fitted parameters are highly interdependent, have extremely large errors, and fluctuate greatly with initial values. Thus, a number of assumptions were made.

First the parameter  $I_2$  was set to zero ( $I_2$  is the Fourier transform of the exchange interaction between two manganese atoms). Considering that these alloys are dilute in manganese, the probability that two manganese atoms will be side by side is much less than for other pairs.

The second assumption was to set  $B_1 = B_2 = B$ . This was done as the atoms are very similar, that is they are transition metal atoms very close to one another on the periodic table. As  $B$  is merely a constant such that  $\alpha/B$  gives the saturating moment of an atom, it was deemed reasonable to make  $B_1$  and  $B_2$  equivalent. As a result equation (6) becomes

$$\bar{m} = \frac{a_2(0) + A_2(0)}{B} + c \left( \frac{a_1(0) - a_2(0) - 2A_2(0)}{B} \right) + c^2 \left( \frac{A_1(0) + A_2(0)}{B} \right) - \frac{1}{B[c^2 I_1(0) + 2c(1-c) I_{12}(0)]}. \quad (9)$$

To further reduce the parameters, a value for  $BI_1 = 0.444$  was assumed, and the expression was then fitted. Convergence was much more rapid and the parameters obtained had less error and were not dependent on initial values. The value for  $BI_1$  was then confirmed by fitting with different values of  $BI_1$ . The fitted and separated values for the parameters obtained from the fit appear in Table 2.

Table 2. Fitted and separated parameters

Parameter	Value	Parameter	Value
$(a_2 + A_2)B^{-1}$	$-4.056^A$	$a_1(0)B^{-1}$	$3.924^B$
$(a_1 - a_2 - 2A_2)B^{-1}$	$9.780^A$	$a_2(0)B^{-1}$	$-2.256^B$
$(A_1 + A_2)B^{-1}$	$-1.723^A$	$A_1(0)B^{-1}$	$0.077^B$
$BI_1$	$0.444^A$	$A_2(0)B^{-1}$	$-1.800^B$
$BI_{12}$	$0.832^A$		

<sup>A</sup> Value obtained by fitting equation (6).

<sup>B</sup> Value obtained by matching the species' moments for dilute Mn to those calculated by Cable (1982).

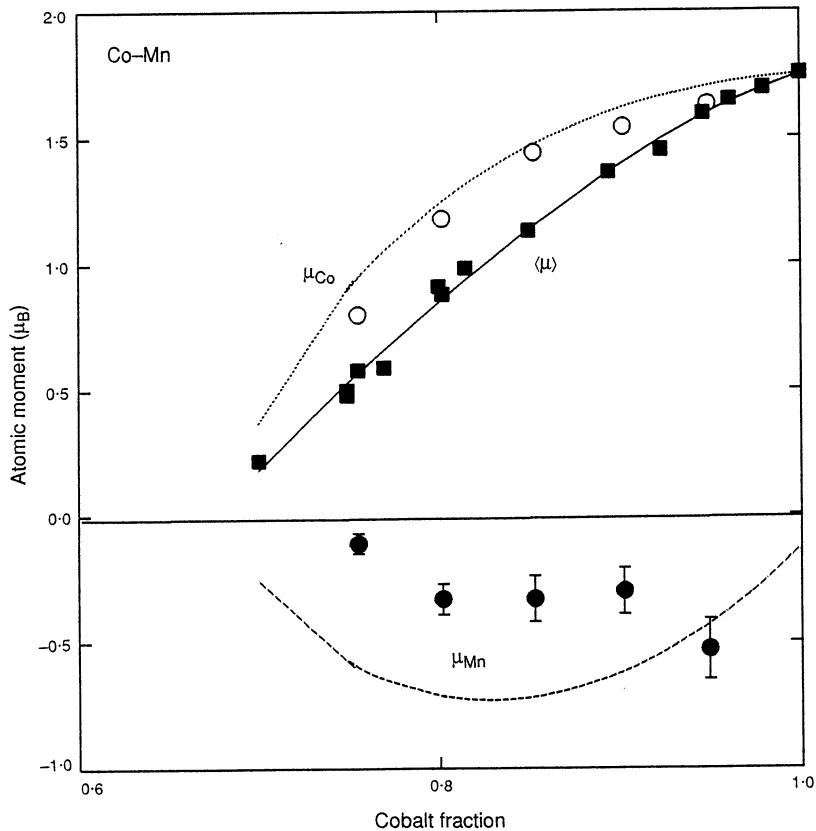


Fig. 2. Mean moments on the two species as calculated here (curves) and from the measurements of Cable (1982).

Equation (8) was used in the separation of the parameters in that by calculating the difference in moment, we were able to calculate the mean moment on each atomic species in the system. By fitting the results to the moments calculated by Cable (1982), we were able to fix a result for  $A_2(0)B^{-1}$ , and thus separate the other parameters (see Fig. 2).

The fitting of Cable's data for the average moments on the two species was done by eye, and while the correspondence between the cobalt moments is good, there is a discrepancy between the manganese moments as calculated here and those calculated by Cable. Not only do the points not correspond, but the general trend of the two sets of results differs. Regarding this discrepancy it is worth noting that changing the values of the parameters does not significantly change the general trend of the results calculated here. The magnitudes of the calculated values do vary, however, and this puts constraints on the parameters.

The fact that the trend in the results does not change with changes in the parameters gives us confidence in our results, and from all appearances the results are physical and believable. As stated before, these samples suffer at low manganese concentration from hcp contamination. Great care was taken in ensuring that the data used in this paper was from 100% fcc samples. Cable (1982) did state that his samples were between 40% and 50% fcc over the composition range, and perhaps it is possible that hcp contamination in the sample dilute in Mn would account for the discrepancy between the two results.

To predict the form of the neutron cross sections, further assumptions had to be made about the ranges of  $A(\kappa)$  and  $I(\kappa)$ . The first assumption was that at these concentrations, any change in susceptibility will be a very local effect. The reasoning behind this is simple: in a metal, if an atom of type 2 is put into an environment of type 1 atoms, the electrons from surrounding atoms will screen any charge difference. This effect is unlikely to stretch any further than the first neighbours. Indeed, a calculation of the Thomas-Fermi screening radius gives a value of approximately 2.4 Å, whereas the nearest-neighbour distance is 2.55 Å. The atomic magnetic susceptibility is a result of the electron structure of that atom. Thus, to a good approximation, the addition of a foreign atom to a system will affect the susceptibility of first neighbours only. We therefore assumed that  $A(\kappa)$ , the Fourier transform of the susceptibility, involved nearest neighbours only. In a centrosymmetric structure (such as fcc)  $A(\kappa)$  will be an even function:

$$A(\kappa) = A(0) [1 - z\kappa^2], \quad (10)$$

for small  $\kappa$ , where  $z$  is a function of the squared product of the number of first neighbours with the distance to the first nearest neighbour.

The same cannot be said of the exchange interactions,  $\zeta(\mathbf{R})$ , which essentially constitute a potential. There are arguments to suggest that the interactions with atoms many atomic distances away should be considered (e.g. RKKY interactions). For simplicity, however, we have only considered these interactions to a maximum distance of the second-nearest neighbour. An initial calculation showed that considering only first-neighbour interactions gave the wrong  $\kappa$ -dependence. Note that  $I(\kappa)$  is also even and it can also be expanded for small  $\kappa$  with a term quadratic in  $\kappa$ .

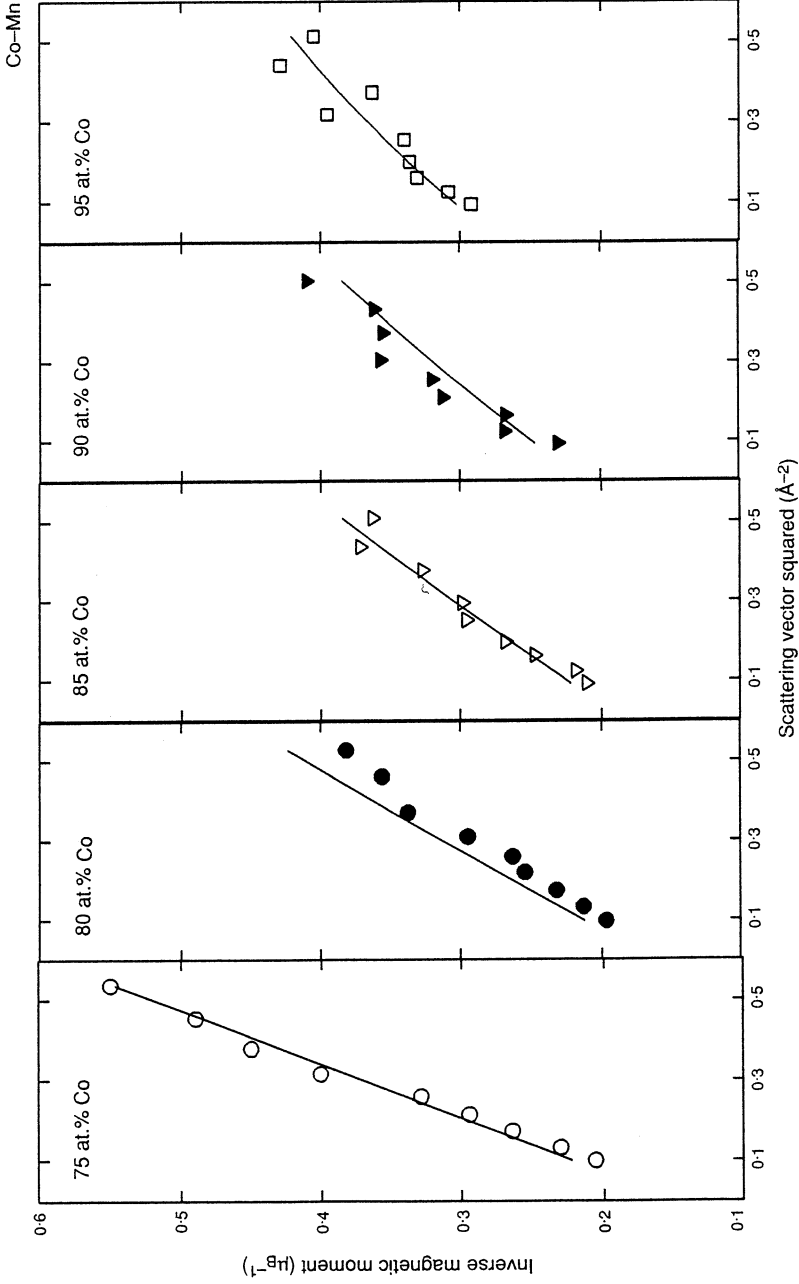


Fig. 3. Calculated moment disturbance function compared with the small- $\kappa$  values from the experimental measurements of Cable (1982).

A point to note is that by introducing the above assumptions we find that  $M(\kappa)$  now has a factor that is Lorentzian in  $\kappa$ , which dominates the  $\kappa$  dependence as  $\bar{m} \rightarrow 0$ . In the comparison of our moment disturbance functions with those of Cable (1982) we have thus plotted  $M(\kappa)^{-1}$  against  $\kappa^2$  in the hope that we would be dealing with straight line plots.

Once the parameters were obtained and the functions  $A(\kappa)$  and  $I(\kappa)$  specified, it was a simple matter to substitute them into equation (7) to find  $M(\kappa)$ . This function has a direct correspondence with the moment disturbance functions plotted in Cable's (1982) paper. Before we could attempt a comparison, however, the important point of atomic short-range order had to be considered.

As shown by Wildes *et al.* (1992) there is significant atomic short-range order contributing to the neutron cross sections at 32 and 37 at.% Mn. There is every reason to believe that a similar cross section exists at lower concentrations of manganese. Cable (1982) has plotted a moment disturbance function that assumes no atomic short-range order. We have thus made a simple correction by multiplying Cable's data by a short-range order function

$$\frac{1}{M_P(\kappa)} = \frac{1}{M_C(\kappa)} \left( 1 + \xi \frac{\sin(\kappa R_1)}{\kappa R_1} \right),$$

where  $M_P(\kappa)$  is the corrected and plotted value (see Fig. 3),  $M_C(\kappa)$  is the value read from Cable's plots, and  $\xi$  is a short-range order parameter estimated by extrapolation of the moment disturbance function to  $\kappa = 0$  and equating it to  $d\bar{m}/dc$ . The values of  $\xi$  for the different concentrations are given in Table 3.

**Table 3. Short-range order parameters used for each concentration**

Mn conc. (at.%)	5.0	9.7	14.7	19.8	24.4
Short-range order parameter, $\xi$	0.479	0.079	-0.194	-0.409	-0.500

Note that in the above equation we are considering  $[M(\kappa)]^{-1}$ . This is because, as noted before, we are plotting  $[M(\kappa)]^{-1}$  versus  $\kappa^2$  in the hope of observing straight line plots. Fig. 3 shows the small- $\kappa$  data of Cable (1982) corrected for atomic short-range order. The small- $\kappa$  cross section is isotropic, so that the polycrystalline data of Cable can be used. The fact that the data for each concentration lie approximately on a straight line is a sign that confidence may be placed in the magnetic environment model.

Fig. 3 also shows for comparison the  $[M(\kappa)]^{-1}$  calculated using the magnetic environment model. For all five compositions the model compares well with the experimental data. This in itself adds justification to the assumptions made at the beginning of the modelling.

#### 4. Discussion

The satisfactory comparison of the experimental data with the results obtained from the magnetic environment model is the result of a number of assumptions and simplifications. Each has been discussed in the text and each has some

physical justification. Putting aside the precise values of the parameters that go into the calculation, the applicability of the magnetic environment model must be justified by the clear Lorentzian dependence of the cross section on  $\kappa$ , and the increase in the correlation length as the critical concentration is approached.

Some confidence in the derived parameters is provided by the similarity of the absolute values of the slopes in Fig. 3 for *all* concentrations. However, further discussion of the parameters should wait until the model has been applied to other cobalt alloys with some of the parameters in common with this system.

## 5. Conclusion

From mean magnetic moment versus concentration data for Co-rich Co-Mn alloys, the magnetic environment model was used to find *various parameters*. These were then used to predict the moment disturbance functions for different compositions of Co-Mn, and these were matched against the experimental data of Cable (1982). The theory fitted experiment quite well. In order for this to happen, however, a number of assumptions had to be made in order to obtain believable and reproducible values for the parameters. These assumptions were physically reasonable, and we believe that they in no way compromised the fit or the success of the model.

## Acknowledgments

This work was completed with the financial assistance of the ARC and AINSE. A. R. Wildes receives a Monash Departmental Scholarship.

## References

- Balcar, E., and Marshall, W. (1968). *J. Phys.* C 1, 966.
- Cable, J. W. (1982). *Phys. Rev.* B 25, 4670.
- Crangle, J. (1957). *Phil. Mag.* 2, 659.
- Hicks, T. J. (1977). *J. Phys.* F 7, 481.
- Hicks, T. J. (1980). *J. Phys.* F 10, 879.
- Hicks, T. J., and Moze, O. (1981). *J. Phys.* F 11, 2633.
- Johnson, D. D., Pinski, F. J., and Stocks, G. M. (1985). *J. Appl. Phys.* 57, 3018.
- Kouvel, J. S. (1960). *J. Phys. Chem. Solids* 16, 107.
- Marshall, W. (1968). *J. Phys.* C 1, 88.
- Matsui, M., Ido, T., Sato, K., and Adachi, K. (1970). *J. Phys. Soc. Jpn* 28, 791.
- Medina, R. A., and Cable, J. W. (1977). *Phys. Rev.* B 15, 1539.
- Men'shikov, A. Z., Takzei, G. A., Dorofeev, Yu. A., Karantsev, V. A., Kotstyshin, A. K., and Sych, I. I. (1985). *Sov. Phys. JETP* 62, 107.
- Nakai, Y., Hozaki, K., and Kunitomi, N. (1978). *J. Phys. Soc. Jpn* 45, 73.
- Wildes, A. R., Kennedy, S. J., Cussen, L. D., and Hicks, T. J. (1992) *J. Phys. Condens. Matter* 4, 8961.

